Journal of Solid State Chemistry 184 (2011) 3158–3162

Contents lists available at SciVerse ScienceDirect

Journal of Solid State Chemistry

journal homepage: www.elsevier.com/locate/jssc

$BaSn_6Co_6O_{19}$—A novel frustrated antiferromagnet with the magnetoplumbite type structure

L. Shlyk, R. Niewa *

Institut für Anorganische Chemie, Pfaffenwaldring 55, 70569 Stuttgart, Germany

ARTICLE INFO

Article history:
Received 2 July 2011
Received in revised form
11 September 2011
Accepted 22 September 2011
Available online 4 October 2011

Keywords:
Magnetoplumbite
Frustrated antiferromagnetism
Kagome lattice

ABSTRACT

Single crystals of the novel compound $BaSn_6Co_6O_{19}$ with maximum width 1 mm and thickness around 0.05 mm were grown from a barium chloride flux. The composition was determined from refinements of single crystal X-ray diffraction data and microprobe analysis. $BaSn_6Co_6O_{19}$ crystallizes in the magnetoplumbite type structure (hexagonal, space group $P6_3/mmc$, $a=6.0940(1)$ Å, $c=23.9633(5)$ Å, $V=770.69$ Å^3, $Z=2$). A significant disorder is generated by random occupation of two octahedrally coordinated crystallographic sites with Co^{2+} and Sn^{4+} ions, while further sites are exclusively occupied by either Co^{2+} (tetrahedrally coordinated) or Sn^{4+} (octahedrally coordinated). One site with mixed occupation realizes the topology of a kagome net. The temperature dependence of the magnetic susceptibility for a single crystal $BaSn_6Co_6O_{19}$ reveals a low temperature antiferromagnetic order at $T_N=14$ K. A relatively large value of frustration factor $f_{//}=|\Theta_{W//}|/T_N\approx 26$ and $f_{\perp}=|\Theta_{W\perp}|/T_N\approx 12$ implies a frustrated antiferromagnetism.

1. Introduction

Transition metal oxides continue to attract great attention in solid state physics and chemistry. In particularly, cobalt oxide based materials has been actively investigated, primarily because they exhibit a wide variety of unusual magnetic and electronic properties. Recently, a number of cobalt oxide materials have been synthesized which display a fascinating diversity of behavior including various forms of charge, spin and orbital ordering. Obvious examples are perovskites $La_{1-x}A_xCoO_3$ (A=Ca, Sr, Ba) [1], $LnBaCo_2O_{5+x}$ (Ln=Eu, Gd) [2,3], $LnCoO_3$ (Ln=La, Dy) [4] possessing giant magnetoresistivity and anomalously high thermoelectric effect, and the recently discovered superconductor $Na_xCoO_2\cdot yH_2O$ ($T_c=5$ K) [5]. In an attempt to explore the formation of new oxocobaltates we have investigated the synthesis and crystal growth of Co bearing members of the magnetoplumbite structure. This large family is composed of magnetoplumbite-related members, i.e. $AFe_{12}O_{19}$, where A=Pb, Ca, Sr, Ba, which is a very important class of magnetic oxides. Some representatives of this family such as Sr- and Ba-bearing ferrites possess extraordinary magnetic properties, which make them excellent materials for use as permanent magnets, recording media, and as components in microwave devices. Within this structural family the A^{2+} ion can also be replaced by trivalent ions of about the same size, e.g., by Ln^{3+} (from La^{3+} to Eu^{3+}) or by Al^{3+}(Ga^{3+}) ions, which leads to a new family of magnetoplumbite type oxides exhibiting interesting optical properties [6,7]. The transition metal atoms may also be substituted by a variety of different metal species, for example, in $SrFe_{12}O_{19}$, Fe^{3+} can be partially replaced by Cr^{3+}, leading to solid solutions $SrFe_{12-x}Cr_xO_{19}$ ($0<x<8$) (Ref. [7] and references therein). The magnetic ground state of these solutions varies from long-range magnetic order to spin-glass freezing with increasing x. Furthermore, magnetic Fe^{3+} can be replaced by nonmagnetic Ga^{3+}, therefore, yielding $SrGa_{12-x}Cr_xO_{19}$ ($0\le x<1$) (SCGO), which is a quasi-2D insulator with an extreme degree of magnetic frustration ($|\Theta_{W||}|/T_f>117$) [8]. This compound attracted a considerable theoretical and experimental interest in attempts to clarify the properties of geometrically frustrated systems. Apart from the Fe-bearing ferrimagnets mentioned above, frustrated antiferromagnets seem to have no practical use, but they are of interest from the point of view of fundamental science since they demonstrate various intriguing low-temperature phenomena such as spin-liquid, spin-glass and spin-ice state [9–11]. Note here, that the magnetoplumbite type crystal structure may be considered to consist of alternating spinel ($S=M_6O_8^{2+}$) and hexagonal stacked ($R=AM_6O_{11}^{2-}$) layers, where M is a transition metal in +3 oxidation state. The structural $AM_6O_{11}^{2-}$ units contain a kagome lattice of the transition metal ions within the ***ab***-plane, suggesting the possibility of geometrical frustration at low temperatures when spins of M are coupled antiferromagnetically. It is believed that frustration in SCGO is associated with two-dimensional kagome layers of antiferromagnetically coupled Cr^{3+} ($S=3/2$) ions. In spite of the very high Curie–Weiss temperature of SCGO, $\theta_{CW}\approx -500$ K, the temperature of the actual spin glass freezing was found to be very low $T_g=3.3$ K. Furthermore, it is shown that the low-temperature specific heat of SCGO is proportional to T^2, instead of usual linear T dependence of spin glasses [12]. These anomalous properties imply that a new type of spin excitations exist on the kagome planes of SCGO [13].

* Corresponding author. Fax: +49 711/685 64241.
E-mail address: rainer.niewa@iac.uni-stuttgart.de (R. Niewa).

0022-4596/$ - see front matter © 2011 Elsevier Inc. All rights reserved.
doi:10.1016/j.jssc.2011.09.028

Up to our knowledge the formation of the magnetoplumbites $ACo_{12}O_{19}$ was not reported up to date. It occurred to us that they might be stabilized by the combination of Co^{2+} and Sn^{4+} in an equimolar amount. Therefore, we successfully synthesized the novel magnetoplumbite $BaSn_6Co_6O_{19}$. The crystal structure contains kagome layers of antiferromagnetically coupled Co^{2+} ions, separated by further Co^{2+} containing layers. Disorder in this compound stems from the dilution of the magnetic Co^{2+} sub-lattice by nonmagnetic Sn^{4+}. These structural features are similar to those of SCGO. As a consequence $BaSn_6Co_6O_{19}$ reveals a behavior characteristic of frustrated antiferromagnets.

We have recently developed a technique for single crystal growth of Ba containing *R*-type ferrites from a $BaCl_2$ flux [14–16]. We have adapted this method to grow single crystals of $BaSn_6Co_6O_{19}$ up to 1 mm in size sufficient for structure determination and detailed studies of magnetic properties. Herein we report crystallographic data of this new phase, together with magnetic measurement data, which have been unavailable in literature.

2. Experimental

For single crystal growth of $BaSn_6Co_6O_{19}$ initial amounts of 2.7 mmol SnO_2, 2 mmol Co_3O_4 and 3.2 mmol $BaCl_2$ were mixed and then pressed into a pellet. The final pellet was heated to 1320 °C and kept at this temperature for several days. Then the furnace was slowly cooled to room temperature. Black hexagonal platelets with maximal sizes of 1 mm and thickness of about 0.05–0.07 mm were obtained. For X-ray diffraction intensity data collection a small black crystal with the shape of hexagonal platelet was selected. The data were collected at ambient temperature using a four circle diffractometer (NONIUS-κ-CCD, Bruker AXS GmbH) with monochromatic Mo*K*α radiation. An absorption correction based on symmetry-equivalent reflections was applied (program X-Shape). The structure was solved using direct methods, and refined in space group $P6_3/mmc$ (no. 194; centrosymmetric, programs Shelxs-97-2, Shelxl-97-2 [17]) leading to a composition of $BaSn_{5.8(2)}Co_{6.2}O_{19}$. Information concerning the data collection and results of the structural refinements for the crystals studied in this work are collected in Tables 1 and 2. Table 3 gathers selected interatomic distances. Further details of the crystal structure investigation can be obtained from the Fachinformationszentrum (FIZ) Karlsruhe, D-76344 Eggenstein-Leopoldshafen, Germany (fax +49(0)7247/808-666; e-mail: crysdata@fiz-karlsruhe.de) on quoting the depository number CSD-423256.

Table 1
Crystal structure data for $BaSn_6Co_6O_{19}$.

Formula	$BaSn_{5.8(2)}Co_{6.2}O_{19}$
Crystal system	Hexagonal
Space group	$P6_3/mmc$
a (Å)	6.0940(1)
c (Å)	23.9633(5)
V (Å^3)	770.69
Z	2
D_{calcd} (g cm^{-3})	6.443
μ(Mo*K*α) (mm^{-1})	18.31
F(000), e	1330.8
hkl range	±8, −7−8, −30−31
$2\theta_{max}$ (deg.)	55.74
Refl. measured	11,026
Refl. unique	401
R_{int}	0.095
Param. refined	44
$R(F)$/w$R(F^2)$ (all reflections)	0.031/0.065
GoF (F^2)	1.273
$\Delta\rho_{fin}$ (e Å^{-3})	2.00

Table 2
Positional parameters for $BaSn_6Co_6O_{19}$. *U*-values given in Å^2.

Atom	Site	x	y	z	U_{eq}
Ba	2*d*	2/3	1/3	1/4	0.0111(3)
M(1)[a]	2*a*	0	0	0	0.0067(6)
Co(2)	2*b*	0	0	1/4	0.0176(6)
Co(3)	4*f*	1/3	2/3	0.02618(6)	0.0080(4)
Sn(4)	4*f*	1/3	2/3	0.18942(3)	0.0052(3)
M(5)[a]	12*k*	0.16588(4)	2*x*	0.89507(2)	0.0070(3)
O(1)	4*e*	0	0	0.1513(3)	0.007(1)
O(2)	4*f*	1/3	2/3	0.9416(3)	0.005(1)
O(3)	6*h*	0.1874(6)	2*x*	¼	0.009(1)
O(4)	12*k*	0.1532(4)	2*x*	0.0536(2)	0.010(1)
O(5)	12*k*	0.5048(4)	2*x*	0.1508(2)	0.007(1)

[a] Occupation of *M*(1)=0.296(5) Sn, 0.704 Co; *M*(5)=0.584(3) Sn, 0.416 Co.

Table 3
Selected distances (Å) for $BaSn_6Co_6O_{19}$, with estimated standard deviations in parentheses.

Ba–O(5)	2.927(4)	6 ×
Ba–O(3)	3.0548(4)	6 ×
M(1)–O(4)	2.065(5)	6 ×
Co(2)–O(3)	1.978(6)	3 ×
Co(2)–O(1)	2.366(7)	2 ×
Co(3)–O(4)	2.013(4)	3 ×
Co(3)–O(2)	2.026(8)	1 ×
Sn(4)–O(5)	2.032(4)	3 ×
Sn(4)–O(3)	2.117(5)	3 ×
Sn(4)–Sn(4)	2.904(1)	1 ×
M(5)–O(5)	2.058(3)	2 ×
M(5)–O(1)	2.074(4)	1 ×
M(5)–O(4)	2.088(3)	2 ×
M(5)–O(2)	2.090(4)	1 ×

Chemical μ-probe analyses result in very consistent compositions observed for all crystals investigated, and the inferred atomic density ratios $n(Ba)/n(Sn)/n(Co)=1.02\pm4:6.04\pm7:5.96\pm7$ (the oxygen content could not be quantified with this technique), is in excellent agreement with the composition $BaSn_{5.8(2)}Co_{6.2}O_{19}$ inferred from the X-ray diffraction data. No additional elements were detected. The X-ray diffraction and microprobe results indicate the single crystals examined were single phase and of excellent quality. The magnetization data for oriented single crystals were acquired over a temperature range $2\ K\le T\le 300\ K$ in applied magnetic fields $0\le\mu_o H\le 5\ T$ using a Quantum Design MPMS7 Magnetometer. The ac magnetic susceptibility was measured with an amplitude of 5 Oe and at frequencies 20, 215, 900 Hz.

3. Results and discussion

3.1. Crystal structure and composition

$BaSn_6Co_6O_{19}$ crystallizes in the hexagonal space group $P6_3/mmc$ in the well known structure of magnetoplumbite $PbFe_{12}O_{19}$ [18,19] (Fig. 1). As usual for ferrites the crystal structure of $BaSn_6Co_6O_{19}$ can be traced down to a closed packed motif with cubic and hexagonal stacking in the sequence **BAB′ABCAC′AC** along the [001] direction. In this sense, the layers **A**, **B**, and **C** constitute exclusively from oxide ions, while the layers **B′** and **C′** have the composition BaO_3. Sn and Co occupy voids exclusively formed by oxide ions. The structure can be partitioned into two alternating sections: spinel-like blocks (so-called *S*-blocks) with cubic stacking sequence of close packed layers and blocks with hexagonal stacking sequence (so-called *R*-blocks). In the spinel-like blocks three layers of edge-sharing octahedral voids are filled with mixed

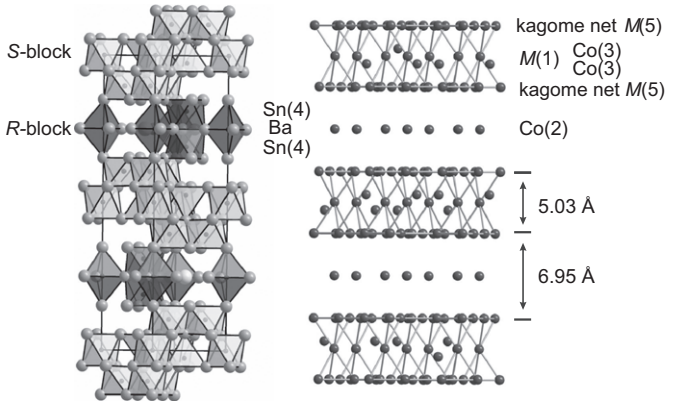

Fig. 1. Crystal structure of $BaSn_6Co_6O_{19}$ emphasizing the interconnection of metal centered oxide polyhedra (left, unit cell is indicated) and arrangement of sites with occupation by Co (right, sites exclusively occupied by Ba, O or Sn are omitted for clarity). Interatomic distances below 3.10 Å are indicated by lines. Distances indicate spacings between Kagomé nets.

occupation of Sn and Co ($M(1)$ and $M(5)$) with different preference for the two metal species. In the middle part of the spinel-like block additional tetrahedral voids, which share vertices with the aforementioned octahedra are exclusively filled with Co(3) (compare Fig. 1). In the *R*-blocks with hexagonal sequence of closed packed layers doubles of face-sharing octahedra occur, which are exclusively occupied with Sn(4). Since in face-sharing octahedra naturally short distances between central atoms occur, it may surprise that Sn^{4+} occupies this position, whereas there is no indication for any significant Co occupation of this site from structure refinements. However, the observed distance d(Sn(4)–Sn(4))=290.4(1) pm is only less than 15 pm shorter than distances between Sn atoms located in edge-sharing octahedra within the *S*-block (Sn(5)–Sn(5), Sn(1)–Sn(5)), as a result from displacement of Sn(4) from the ideal central position of the octahedra. This displacement is indicated by the elongated distances to the bridging oxide ions of the Sn_2O_9-unit with d(Sn(4)–O(5))=211.7(5) pm as compared to the terminal oxide ions with d(Sn(4)–O(5))=203.2(4) pm. The same conclusion can be derived from analysis of the internal angles. Such a preference of Sn for the face-sharing octahedra doubles was earlier observed for example for the isotype $SrSnFe_{11}O_{19}$ [20] or in the *R*-type ferrites $BaFe_{4-2x}Sn_{2+x}Co_xO_{11}$ [21] and $SrSn_2Ga_{1.3}Cr_{2.7}O_{11}$ [22]. Earlier it was argued that the highest charged cation Sn^{4+} tends to occupy the position with the highest coordination number [21], but this reasoning does not take into account the mixed occupancy of $M(5)$ or even the Co-preference at $M(1)$, which are both octaherdrally coordinated. It is worthwhile for the magnetic data discussion to point out that the *S*-block is terminated by two kagome nets of $M(5)$ located in edge-sharing octahedra of oxygen. The refinement of the occupation of the metal site results in about 60% Sn and 40% Co. No indication for any additional Sn–Co long range order could be extracted from the diffraction data. There was also no hint for significant short range order from X-ray diffraction data taken on both single crystals and powder (reflection shapes, diffuse scattering).

Within the *R*-block additionally trigonal bipyramids are occupied exclusively by Co(2). A slight elongation of the displacement parameters in direction of the axial oxide ions ([001] direction) indicates the preference of Co(2) to reside in a tetrahedral coordination rather than a trigonal bipyramidal environment. A refinement with a split position of Co(2) with statistical occupation on both sides of the mirror plane in (001) results in a separation of 37(2) pm (site (1/3, 2/3, 0.2576(4))) with no significant additional changes in the refinement results. Earlier investigations on $SrFe_{12}O_{19}$ and $BaFe_{12}O_{19}$ revealed a dynamical vibration behavior of the respective Fe atom between the tetrahedra at ambient temperature and a constantly decreasing distance between the split positions with decreasing temperatures resulting in a true trigonal bipyramidal coordination at 4.2 K derived from X-ray diffraction and Mössbauer spectroscopy [23,24].

The composition $BaSn_{5.8(2)}Co_{6.2}O_{19}$ results from refinement of the X-ray diffraction intensity data. Provided Ba^{2+}, Sn^{4+} and O^{2-} ions in combination with charge neutrality an average oxidation state of close to +2 calculates for Co, for pure Co^{2+} a composition of $BaSn_6Co_6O_{19}$ within the statistical error of the refinement would result, which is excellent agreement with the composition derived from μ-probe analyses ($Ba_{1.02\pm4}Sn_{6.04\pm7}Co_{5.96\pm7}O_x$). Interestingly, the details in the metal atomic preferences for the different sites differ from those derived from neutron diffraction for $BaTi_6Co_6O_{19}$ [25]: Only for the tetrahedrally coordinated site pure occupation with Co was found, while all other sites are mixed occupied by Co and Ti. Still, the tendencies of occupation factors are similar with the exception of the $M(1)$ position where significantly more Ti is located in $BaTi_6Co_6O_{19}$ (83%) than Sn in $BaSn_6Co_6O_{19}$ (30%). However, these occupation factors for both compounds may be strongly dependent on the thermal history, i.e., the synthesis conditions applied.

3.2. Magnetic properties

Fig. 2 shows data for the magnetic susceptibility $\chi=M/H$ for a $BaSn_6Co_6O_{19}$ single crystal oriented parallel to the **c**-axis in an applied field of $\mu H=0.1$ T. A magnetic transition is indicated by a sharp maximum at $T=14$ K (Fig. 2). A similar behavior of the magnetic susceptibility emerges for $\boldsymbol{H}\perp\mathbf{c}$: an abrupt decrease below 14 K (Fig. 3). The sharp decrease of $\chi_{\perp,\parallel}(T)$ below $T=14$ K is typical of antiferromagnetic state. On the other hand, a structural disorder due to the random replacement of magnetic Co^{2+} by nonmagnetic Sn^{4+} on the $Ba(Sn,Co)_6O_{11}^{4-}$ kagome and $(Sn,Co)_6O_8^{4+}$ spinel sublattices may cause a spin glass freezing at 14 K indicative on short-range type magnetic ordering. The characteristic feature of spin glasses is the irreversibility, i.e. the difference in value and shape between the magnetization versus temperature curves after zero-field cooling (ZFC) and field cooling (FC) at temperatures below the spin freezing temperature.

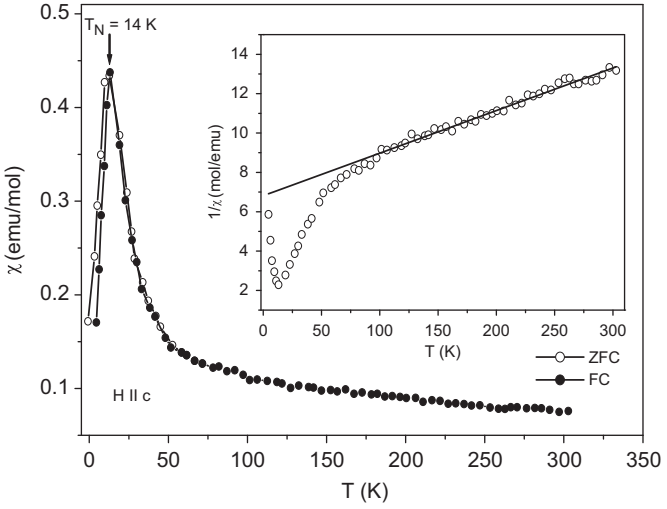

Fig. 2. Temperature dependence of the FC dc magnetic susceptibility $\chi(T)$ of a single crystal $BaSn_6Co_6O_{19}$ for $\boldsymbol{H}\|\mathbf{c}$ at an applied magnetic field $\mu_oH=0.1$ T. The inset shows the inverse magnetic susceptibility vs. temperature. The solid line is a fit of the data to the Curie–Weiss law. The arrow designates the temperature of magnetic ordering $T_N=14$ K.

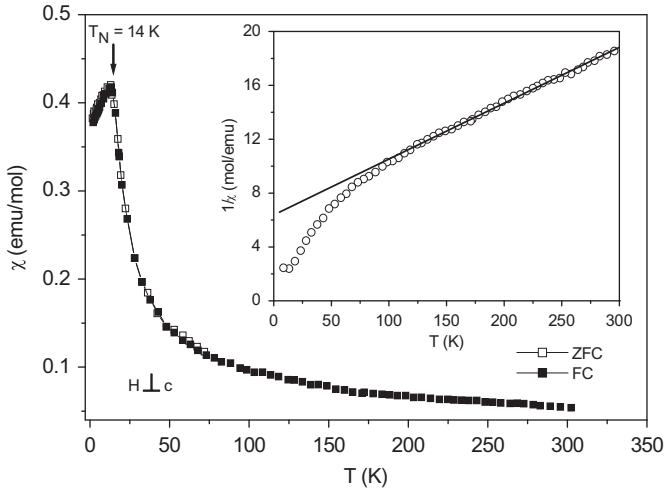

Fig. 3. Temperature dependence of the FC DC magnetic susceptibility $\chi(T)$ of a single crystal $BaSn_6Co_6O_{19}$ for $\boldsymbol{H}\perp\boldsymbol{c}$ at an applied magnetic field $\mu_o H=0.1$ T. The inset shows the inverse magnetic susceptibility vs. temperature. The solid line is a fit of the data to the Curie–Weiss law. The arrow designates the temperature of magnetic ordering $T_N=14$ K.

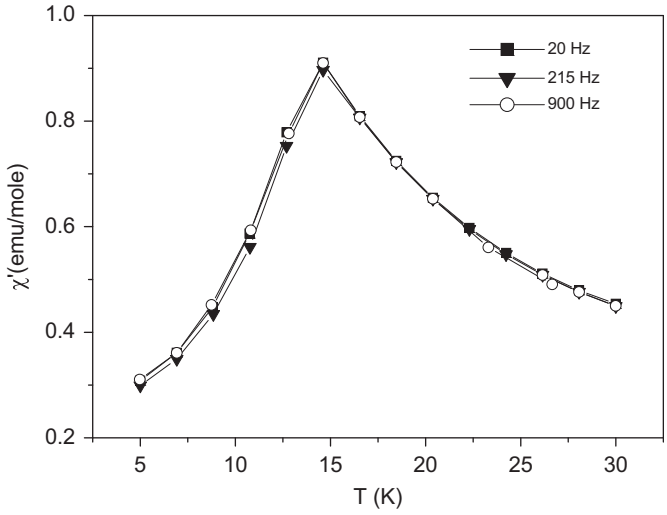

Fig. 4. The real component of the ac susceptibility of a single crystal $BaSn_6Co_6O_{19}$ ($\boldsymbol{H}\|\boldsymbol{c}$) between 30 and 5 K at different frequencies.

The drop of χ below 14 K was further verified by ZFC and field-cooled FC measurements at $\mu H=0.1$ T. As it is seen in Figs. 2 and 3 the ZFC and FC dc χ curves follow each other without significant divergence at low temperatures. This finding is consistent with the onset of long-range magnetic ordering below 14 K. The ac susceptibility can also provide insight on the origin of the peak seen in the dc data. In Fig. 4 the real part of the ac-susceptibility data for $BaSn_6Co_6O_{19}$ is shown at some selected frequencies. There is no observable frequency dependence of the well-defined peak position at $T=14$ K, which always accompanies a true spin glass transition. Therefore, a maximum at 14 K is associated with magnetic transition to a long-range ordered state rather than spin-glass state. The inverse magnetic susceptibility for two crystallographic orientations is shown in the insets of Figs. 2 and 3. The in-plane magnetic susceptibility, $\chi_{\|}(T)$ (inset in Fig. 2), for $T>100$ K follows a Curie–Weiss law $\chi=C/(T-\Theta_W)$ with negative Weiss temperature $\Theta_{W\|}=-365$ K, indicating that Co ions in our sample are very strongly coupled by antiferromagnetic exchange. The effective magnetic moment deduced from the Curie–Weiss fitting is $\mu_{eff}=3.12\mu_B$. This value is slightly lower than that of expected for the high-spin state spin-only moment of $\mu_{eff}=3.87\ \mu_B$ for Co^{2+} (S=3/2). A Curie–Weiss fit to the $\chi_{\perp}(T)$ data over the interval $100\ \text{K}<T<300$ K (inset in Fig. 3) yields a Weiss temperature $\theta_{W\perp}=-169$ K and an effective magnetic moment $\mu_{eff}=2.31\mu_B$, which is lower than the value expected for Co^{2+}. The Curie–Weiss fit, which is taken quite close to the cooperative-ordering transition temperature, may account for the underestimation of the effective magnetic moment. We believe that the anisotropy of the effective magnetic moment is controlled by the large anisotropy of the g-factor expected for Co^{2+} in a noncubic symmetry [26].

To explore further the nature of the low-temperature transition we performed measurements of the magnetic moment, m, versus magnetic field at 5 K. It is obvious from Fig. 5 that the magnetization curves are qualitatively the same for both field orientations, i.e. the isothermal magnetization increases with magnetic field in linear manner without saturation at the maximum applied field of 5 T, showing a weak anisotropy. Furthermore, neither small hysteresis nor remanent magnetization near $H=0$, which could be further evidence for spin glass freezing, is noted in both data sets. This behavior is typical for antiferromagnetic materials. Taking into account the structural peculiarities of the title compound further discussion of the magnetic behavior is worthwhile. The hexagonal structure of $BaSn_6Co_6O_{19}$ (Fig. 1) contains structural subunits with kagome topology $Ba(Sn,Co)_6O_{11}$, which are sandwiched between spinel blocks $(Sn,Co)_6O_8$. The kagome sublatice is a network of metal-centered edge-sharing octahedra with appreciable amount of site disorder between nonmagnetic Sn^{4+} and magnetic Co^{2+} ions: about 60% Sn and 40% Co. The kagome lattice is known to be geometrically frustrated in the presence of nearest-neighbor antiferromagnetic exchange interactions. The degree of the frustration in an antiferromagnet is identified by the ratio of Weiss temperature to the ordering temperature, $f=|\Theta_W|/T_N$. For a frustrated system $f=|\Theta_W|/T_N>10$ is common, in contrast for a non-frustrated magnetically ordered system $T_N\sim\Theta_W$. As it follows from the bulk magnetic measurements of $BaSn_6Co_6O_{19}$ the relatively large anisotropic value of the frustration parameter $f_{\|}=|\Theta_{W\|}|/T_N\approx 26$ and $f_{\perp}=|\Theta_{W\perp}|/T_N\approx 12$ implies a frustrated antiferromagnet. For site-ordered kagome lattice nearest-neighbor antiferromagnetic interactions among Heisenberg spins generate large ground-state degeneracy, but not long-range order. The triangular motif and relatively large separation of the kagome layers (Fig. 1) of $BaSn_6Co_6O_{19}$ would discourage conventional long-range magnetic order. However, weak perturbations, such as lattice disorder [27], anisotropy [28] and next-nearest-neighbor interactions [29],

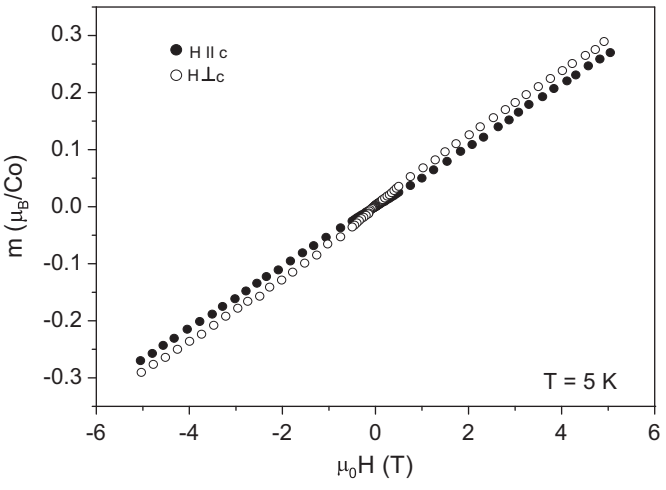

Fig. 5. Magnetic moment m vs. magnetic field H for two crystallographic orientations ($\boldsymbol{H}\|\boldsymbol{c}$ and $\boldsymbol{H}\perp\boldsymbol{c}$) at 5 K of a single crystal $BaSn_6Co_6O_{19}$.

can remove the ground-state degeneracy and induce long-range magnetic order. The above mentioned perturbations are particularly relevant to $BaSn_6Co_6O_{19}$, i.e., the site disorder between the nonmagnetic Sn^{4+} and the magnetic Co^{2+} ions and a large anisotropy expected for Co^{2+}. The observed low-temperature drop in χ suggests that the presence of lattice defects suppress magnetic frustration in $BaSn_6Co_6O_{19}$, favoring the appearance of three-dimensional antiferromagnetic ordering. In this case the compound would be capable of even a higher degree of frustration when Co concentration is increased. However, Co ions in the hypothetical solid solution $BaCo_{12-x}Sn_xO_{19}$ for $x>6$ have to accept mixed or intermediate valence states Co^{2+}/Co^{3+} in order to satisfy charge balance. Unfortunately, our attempts to synthesize $BaCo_{12-x}Sn_xO_{19}$ with $x>6$ failed. Therefore, we conclude that this structure does not stabilize in the presence of trivalent Co under normal conditions. At present is not clear why the system favors long-range order, avoiding spin-glass freezing. This behavior might be due to dominant influence of geometrical frustration of the Co–Co antiferromagnetic exchange on the kagome planes relative to the site disorder of the spinel-like blocks in the formation of the magnetic ground state. To further explore the nature of the magnetic ground state of the novel magnetoplumbite $BaSn_6Co_6O_{19}$, which probably arise from the competition between long-range magnetic order, frustration and disorder effects, a neutron diffraction study with the aim to probe the magnetic structure at low temperatures will be necessary.

4. Conclusion

The present dc and ac magnetic measurements indicate long-range antiferromagnetic order below 14 K in single crystals $BaSn_6Co_6O_{19}$. Despite significant structural disorder generated both in kagome and spinel subunits by random replacement of magnetic Co^{2+} with nonmagnetic Sn^{4+}, the real part of the ac susceptibility does not depend on frequency. This finding offers strong evidence against spin-glass freezing. At 5 K, isothermal magnetization is found to vary linearly without any hysteresis at low fields, which is typical of antiferromagnets. As it follows from the bulk magnetic measurements $BaSn_{5.8}Co_{6.2}O_{19}$ Co^{2+} ions are coupled antiferromagnetically with a magnetic moment of $\mu_{eff}=3.12\mu_B$ and $\mu_{eff}=2.31\mu_B$ along and perpendicular to the ***c***-axis, respectively. From the magnetic point of view $BaSn_6Co_6O_{19}$ is a representative of a system of kagome planes with intervening dilute triangular Heisenberg planes. The frustration factor $f_{\parallel}=|\Theta_{W\parallel}|/T_N\approx 26$ and $f_{\perp}=|\Theta_{W\perp}|/T_N\approx 12$, which is higher than 10 indicates on strongly frustrated antiferromagnetism. It is worth to note that the magnetic data suggest the magnetic moments may preferentially be aligned along the ***c***-axis. This is consistent with the fact that all magnetic ions with the exception of $M(5)$, which is a mixed Sn/Co site, reside at sites whose point group symmetry constrains the moments on these ions to lie along a preferred axis. Neutron diffraction investigations of the magnetic structure are needed to confirm this prediction.

Acknowledgments

We would like to thank Dr. Falk Lissner for collecting the X-ray diffraction data and Klaus Wolff for the EDX measurements. Additionally, we gratefully acknowledge the use of a SQUID magnetometer located in the group of Prof. Martin Dressel and support by Dr. Lapo Bogani.

References

[1] G. Briceno, H.Y. Chang, X.D. Sun, P.G. Schultz, X.D. Xiang, Science 270 (1995) 273–275.
[2] A. Maignan, C. Martin, D. Pelloquin, N. Nguyen, B. Raveau, J. Solid State Chem. 142 (1999) 247–260.
[3] A.A. Taskin, A.N. Lavrov, Y. Ando, Phys. Rev. B 73 (2006) 121101R.
[4] Z. Jirak, J. Hejtmanek, K. Knizek, M. Veverka, Phys. Rev. B 78 (2008) 014432.
[5] K. Takada, H. Sakurai, E. Takayama-Muromachi, F. Izumi, R.A. Dilanian, T. Sasaki, Nature 422 (2003) 53–55.
[6] A. Aharoni, M. Schieber, Phys. Rev. 123 (1961) 807–809.
[7] R. Collongues, D. Gourier, A. Kahn-Harari, A.M. Lejus, J. Thery, D. Vivien, Annu. Rev. Mater. Sci. 20 (1990) 51–82.
[8] X. Obradors, A. Labarta, A. Isalgue, J. Tejada, J. Rodriguez, M. Pernet, Solid State Commun. 65 (1988) 189–192.
[9] A.P. Ramirez, in: K.J.H. Buschow (Ed.), Handbook on Magnetic Materials, vol. 15, Elsevier, Amsterdam, 2001, p. 423.
[10] S.-H. Lee, C. Broholm, W. Ratcliff, G. Gasparovich, Q. Huang, T.H. King, S.-W. Cheong, Nature 418 (2002) 856–858.
[11] S.T. Bramwell, M.J.P. Gingras, Science 294 (2001) 1495–1501.
[12] A.P. Ramirez, G.P. Espinosa, A.S. Cooper, Phys. Rev. Lett. 64 (1990) 2070–2073.
[13] J.T. Chalker, P.C.W. Holdsworth, E.F. Shender, Phys. Rev. Lett. 68 (1992) 855–858.
[14] B. Schüpp-Niewa, L. Shlyk, S. Kryukov, L.E. De Long, R. Niewa, Z. Naturforsch. B 62 (2007) 753–758.
[15] L. Shlyk, S. Kryukov, B. Schüpp-Niewa, R. Niewa, L.E. De Long, Adv. Mater. 20 (2008) 1315–1320.
[16] R. Niewa, L. Shlyk, B. Schüpp-Niewa, L.E. De Long, Z. Anorg. Allg. Chem. 636 (2010) 331–336.
[17] G.M. Sheldrick, SHELXS-97-2, SHELXL-97-2, Universität Göttingen, Göttingen, Germany, 1997.
[18] G. Aminoff, Arkiv Kemi, Mineral. Geol. A12 (1938) 1217.
[19] W.D. Townes, J.H. Fang, A.J. Perrotta, Z. Kristallogr. 125 (1967) 437–449.
[20] P. Sonne, Hk. Müller-Buschbaum, J. Alloys Compd. 199 (1993) L9–L11.
[21] B. Martínez, F. Sandiumenge, I. Golosovski, S. Galí, A. Labarta, X. Obradors, Phys. Rev. B 48 (1993) 16440–16448.
[22] I.D. Posen, T.M. McQueen, A.J. Williams, D.V. West, Q. Huang, R.J. Cava, Phys. Rev. B 81 (2010) 134413.
[23] X. Obradors, A. Collomb, M. Pernet, J. Solid State Chem. **56** (1985) 171–181.
[24] J. Fontcuberta, W. Reiff, X. Obradors, J. Phys.: Condens. Matter 3 (1991) 2131–2136.
[25] M.V. Cabañas, J.M. Gonzáles-Calbet, J. Rodríguez-Carvajal, M. Vallet-Regi, J. Solid State Chem. 111 (1994) 229–237.
[26] A. Abragam, B. Bleaney, Electron Paramagnetic Resonance of Transition Ions, Clarendon Press, Oxford, 1970.
[27] J.E. Greedan, J. Mater. Chem. 11 (2001) 37–53.
[28] C.L. Henley, Phys. Rev. Lett. 62 (1989) 2056–2059.
[29] A. Kuroda, S. Miyashita, J. Phys. Soc. Jpn. 64 (1995) 4509–4512.